Springer

KSME

Journal of Mechanical Science and Technology 29 (2) (2015) 759~767
www.springerlink.com/content/1738-494x
DOI 10.1007/s12206-015-0137-7

Development of a rotary clap mechanism for positive-displacement rotary pumps: Kinematic analysis and working principle†

Sung Bo Shim[1], Young Jun Park[2], Jong Mun Kim[3] and Kyeong Uk Kim[1,*]

[1]*Department of Biosystems & Biomaterials Science and Engineering, Seoul National University, Seoul, 151-921, Korea*
[2]*Korea Institute of Machinery and Materials, Daejeon, 305-343, Korea*
[3]*ClapMC Co. Ltd., Daejeon, 305-343, Korea*

(Manuscript Received April 29, 2014; Revised October 2, 2014; Accepted November 5, 2014)

Abstract

A five-bar spatial mechanism named as a rotary clap mechanism is developed as a pumping device for positive displacement rotary pumps. The mechanism comprises a driving crank, a shaft link with two pins and two gears mounted on the middle and both ends, two rotors with jaws equally spaced along their circumferences, and two fixed internal gears. As the crank rotates, the gear pin-jointed to the crank rotates about the crank pin and at the same time rotates about the center of the fixed internal gears like a hypo-cyclic gear train. The gear-attached shaft link also rotates about the crank pin and about the fixed internal gears at the same time. This motion of the shaft link makes the pins rotate about the center of the fixed internal gears with a periodically varying radius. Therefore, two rotors driven by the pins rotate with different angular velocities. One rotor alternately leads and lags relative to the other rotor. These lead–lag motions between the two jaws of the rotors, which result in suction and discharge required for pumping, resemble hand clapping from which the mechanism was named. Construction and design parameters of the rotary clap mechanism are introduced, and kinematic analysis of this mechanism is performed. The relationships among design parameters, inherent constraints, and effects of design parameters on the displacement of mechanism are also presented.

Keywords: Hypo-cycle mechanism; Kinematic analysis; Rotary clap mechanism; Rotary pump

1. Introduction

Pumping in the conventional rotary pumps takes place when the clearance is created between the rotating elements and pump housing that moves the fluid. As the pump continues to rotate, the motion of the fluid captured by the clearance progresses along the way and the rotating element forces the fluid out of the pump. Rotary pumps have many advantages including self-priming, relatively smooth discharge, and liquid delivery to high pressures. However, the small clearance between the rotating elements and the pump housing causes disadvantages such as small displacement and excessive wear caused by corrosion.

The slider-crank mechanism has been widely applied to a considerable number of types of pumps such as plunger and piston pumps. However, as the pump speed increases, high levels of vibration and power losses caused by excessive friction between the reciprocating piston and pump housing arise. Numerous attempts have been made to develop rotary machines that will solve these problems [1-6, 9-11]. With the exception of the Wankel engine, none of them were practically successful primarily because of poor sealing and manufacturing techniques. The development of such machines have recently attracted considerable attention again as technological advances present solutions for problems associated with rotary machines.

This study attempted to convert the reciprocating slide-crank mechanism into a rotary version named rotary clap mechanism [7, 8] and apply it to the positive displacement rotary pump, with the purpose of increasing its displacement with less vibration and power loss. The mechanism is a five-bar spatial mechanism where two rotors driven at different angular velocities make the clearance between the rotor jaws alternately open and close, resulting in suction and discharge required for pumping. The paper presents the description, motion analysis, correlation of design parameters, inherent constraints, and performance characteristics of the rotary clap mechanism as a pumping device.

2. Description of mechanism

The rotary clap mechanism is a five-link spatial mechanism comprising a crank as the driving link, a shaft link with two

*Corresponding author. Tel.: +82 2 880 4602, Fax.: +82 2 873 2049
E-mail address: kukim@snu.ac.kr
† Recommended by Associate Editor Jae Cheon Lee

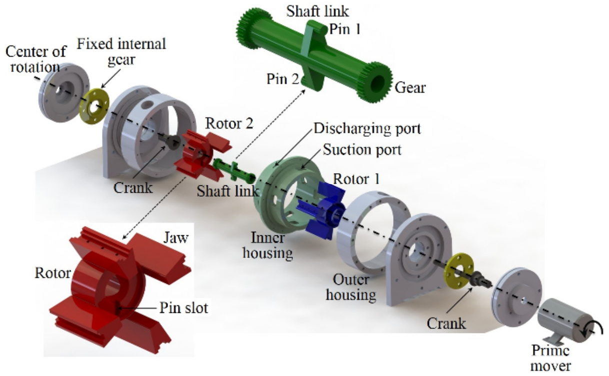

Fig. 1. Structure of rotary clap mechanism as a pumping device.

pins symmetrically located on a plate rigidly mounted in the middle and two gears rigidly attached to both ends, two rotors with jaws equally spaced along their circumferences, and two fixed internal gears. The width of jaw is extended unilaterally twice the rotor width to allow complete engagement of the two rotors jaws. Fig. 1 illustrates the linkages of the mechanism. As the crank rotates, the gear pin-jointed to the crank simultaneously rotates about the crank pin and the center of the fixed internal gears, making the motions of a hypo-cyclic gear train. The shaft link can also simultaneously rotate about the crank pin and about the center of the fixed internal gear. This motion of the shaft link makes the pins rotate about the center of the fixed internal gear with a periodically varying radius. The rotors are driven by the pins on the shaft link through a pin-in-slot joint where the pins move along a radial slot on the contacting faces of two rotors. The angular velocities of the two rotors also change accordingly because the rotational radius of the pin changes as the crank rotates at a constant velocity. The relative velocities of the two rotors results in the periodical lead–lag motion of one rotor with respect to the other. These lead and lag motions result in a continuous cycle of approach–contact–recess of two adjacent rotor jaws, which resembles hand clapping from which the mechanism is named. The continuous lead and lag motions can be used for the suction and discharge motions required for pumping.

3. Motion analysis

3.1 Displacement

Let O-X-Y be a rectangular coordinate with positive x axis to the right, y axis upwards, and its origin at the center of rotors, which also coincides with the center of the fixed internal gear. As the crank rotates counter-clockwise (Fig. 2), the pin-jointed gear simultaneously rotates clockwise with respect to the crank pin and counter-clockwise about the center of the fixed internal gear. Thus, absolute angular displacement of the gear can be expressed as Eq. (1). P_1 and P_2 represent the pins on the shaft link. The position vector equations for the pins can be expressed as Eqs. (2) and (3).

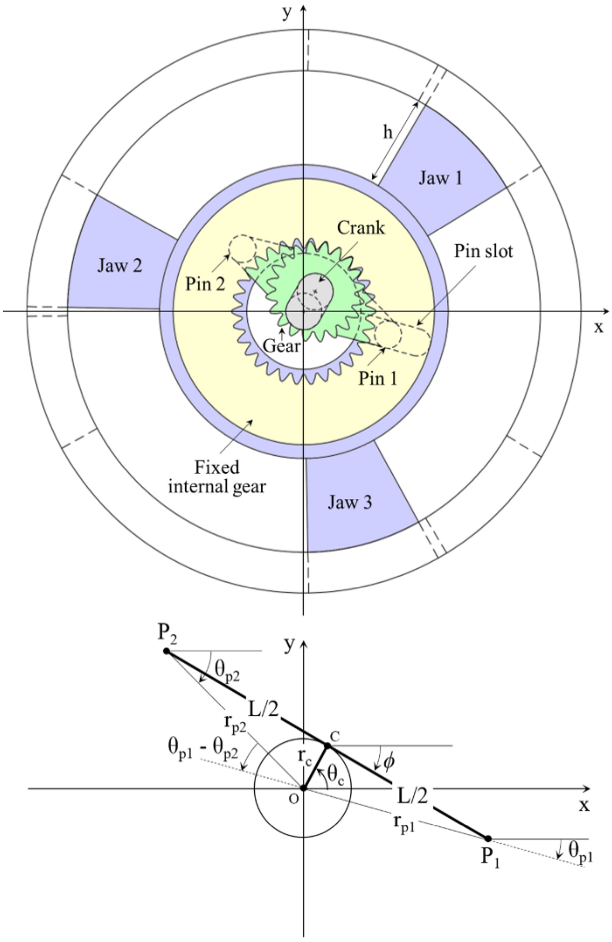

Fig. 2. Motion of the pins relative to the center of the rotors.

$$\phi = \left(1 - \frac{Z_r}{Z_p}\right)\theta_c \tag{1}$$

$$r_c e^{i\theta_c} + \frac{L}{2} e^{i\phi} - r_{p_1} e^{i\theta_{p_1}} = 0 \tag{2}$$

$$r_c e^{i\theta_c} - \frac{L}{2} e^{i\phi} + r_{p_2} e^{i\theta_{p_2}} = 0 \tag{3}$$

where ϕ is the absolute angular displacement of the gear, Z_r is the number of teeth on the fixed internal gear, Z_p is the number of teeth on the gear of shaft link, θ_c is the angular displacement of the crank, r_c is the crank radius, L is the distance between pins P_1 and P_2, r_{p1} is the radius of pin P_1 with respect to the center of rotor O, r_{p2} is the radius of pin P_2 with respect to the center of rotor O, θ_{p1} is the angular displacement of vector $\mathbf{OP}_1$, and θ_{p2} angular displacement of vector $\mathbf{OP}_2$.

Notably, the pins on the shaft link rotate negatively clockwise about the center of the rotors as the crank rotates positively counter-clockwise. In other words, θ_c is positive, whereas ϕ, θ_{p1}, and θ_{p2} are all negative in Eqs. (2) and (3).

Substituting Eq. (1) into Eq. (2) and separating the real and imaginary parts of Eq. (2) yields

$$r_c\cos\theta_c + \frac{L}{2}\cos\left[\left(1-\frac{Z_r}{Z_p}\right)\theta_c\right] = r_{p_1}\cos\theta_{p_1} \tag{4}$$

$$r_c\sin\theta_c + \frac{L}{2}\sin\left[\left(1-\frac{Z_r}{Z_p}\right)\theta_c\right] = r_{p_1}\sin\theta_{p_1} . \tag{5}$$

Solving for r_{p1} yields

$$r_{p_1} = \sqrt{r_c^2 + \frac{L^2}{4} + r_c L\cos\frac{Z_r}{Z_p}\theta_c} . \tag{6}$$

For the clap mechanism to make one complete cycle, the gear on the shaft link must rotate clockwise through $\phi = 2\pi$, and the crank should accordingly rotate counter-clockwise through an angle of $\theta_c = \frac{2\pi Z_p}{Z_r - Z_p}$ radians. Therefore, θ_{p1} can be expressed as Eq. (7) for the first half of the cycle and as Eq. (8) for the second half. In other words,

when $0 \le \theta_c \le \frac{\pi Z_p}{Z_r - Z_p}$

$$\theta_{p_1} = -\cos^{-1}\left[\frac{1}{r_{p_1}}\left\{r_c\cos\theta_c + \frac{L}{2}\cos\left(\left(1-\frac{Z_r}{Z_p}\right)\theta_c\right)\right\}\right] \tag{7}$$

when $\frac{\pi Z_p}{Z_r - Z_p} < \theta_c \le \frac{2\pi Z_p}{Z_r - Z_p}$

$$\theta_{p_1} = -\pi - \cos^{-1}\left[\frac{1}{r_{p_1}}\left\{-r_c\cos\theta_c - \frac{L}{2}\cos\left(\left(1-\frac{Z_r}{Z_p}\right)\theta_c\right)\right\}\right] . \tag{8}$$

Similarly, solving Eq. (3) for r_{p2} and θ_{p2} yields

$$r_{p_2} = \sqrt{r_c^2 + \frac{L^2}{4} - r_c L\cos\frac{Z_r}{Z_p}\theta_c} \tag{9}$$

when $0 \le \theta_c \le \frac{\pi Z_p}{Z_r - Z_p}$

$$\theta_{p_2} = -\cos^{-1}\left[\frac{1}{r_{p_2}}\left\{-r_c\cos\theta_c + \frac{L}{2}\cos\left(\left(1-\frac{Z_r}{Z_p}\right)\theta_c\right)\right\}\right] \tag{10}$$

when $\frac{\pi Z_p}{Z_r - Z_p} < \theta_c \le \frac{2\pi Z_p}{Z_r - Z_p}$

$$\theta_{p_2} = -\pi - \cos^{-1}\left[\frac{1}{r_{p_2}}\left\{r_c\cos\theta_c - \frac{L}{2}\cos\left(\left(1-\frac{Z_r}{Z_p}\right)\theta_c\right)\right\}\right] \tag{11}$$

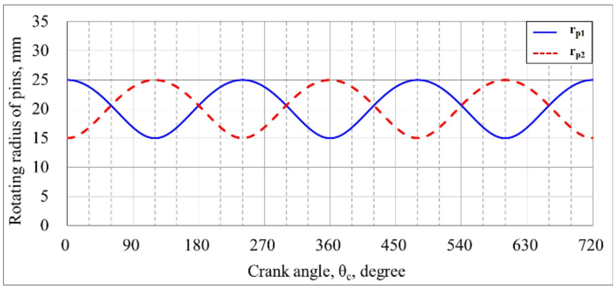

Fig. 3. Rotating radius of pins when $r_c = 5$ *mm*, $L = 40$ *mm*, $Z_r = 30$, and $Z_p = 20$.

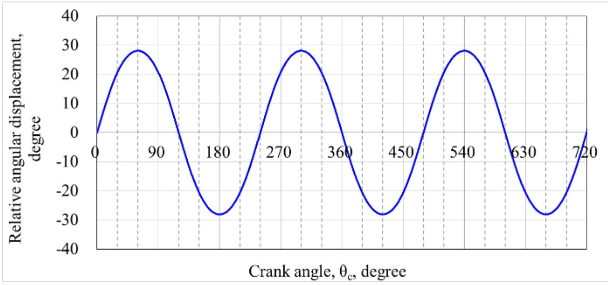

Fig. 4. Relative angular displacement of rotors, θ_{rel} when $r_c = 5$ *mm*, $L = 40$ *mm*, $Z_r = 30$, and $Z_p = 20$.

As the crank rotates with a constant angular velocity, the pins are constrained to simultaneously move along the radial slots on the rotors and rotate about the center of the rotors with r_{p1} and r_{p2} varying periodically with a period of $\tau = 2\pi\frac{Z_p}{Z_r}$. Fig. 3 shows that r_{p1} decreases as r_{p2} increases, and r_{p1} is at a minimum when r_{p2} is at a maximum and vice versa.

When the two rotors having N jaws are assembled, a total of 2 N clearances can be formed by sets of two adjacent jaws and the rotor housing. The volume of the clearance varies with the relative angular displacement, θ_{rel}, of the two rotors, which also varies with a period of $\tau = 2\pi\frac{Z_p}{Z_r}$ as shown in Fig. 4 and determined as

$$\theta_{rel} = \theta_{p_1} - \theta_{p_2} . \tag{12}$$

Then, as the crank rotates, the front and back clearance angles of a jaw can be respectively expressed as follows:

$$\theta_{front} = \left(\theta_{rel}\right)_{\max} - \theta_{rel} \tag{13}$$

$$\theta_{rear} = \left(\theta_{rel}\right)_{\max} + \theta_{rel} . \tag{14}$$

Fig. 5 shows the front and back clearance angles as a function of the crank angle. Notably, the clearance angle varies with a period of $\tau = 2\pi\frac{Z_p}{Z_r}$ so that when two adjacent jaws are in contact, the clearances in the front and back of the two jaws in contact reach the maximum (Fig. 5). Therefore, the maximum values of θ_{front} and θ_{back} are given as

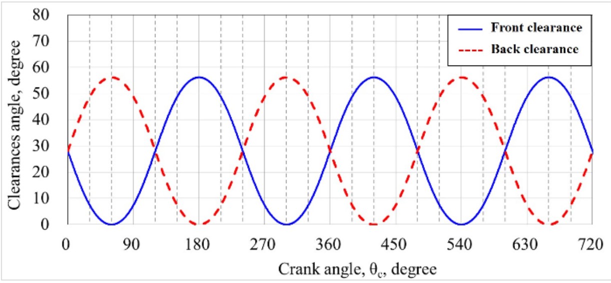

Fig. 5. Clearances angle between two adjacent jaws when r_c = *5 mm*, *L* = *40 mm*, Z_r = *30*, and Z_p = *20*.

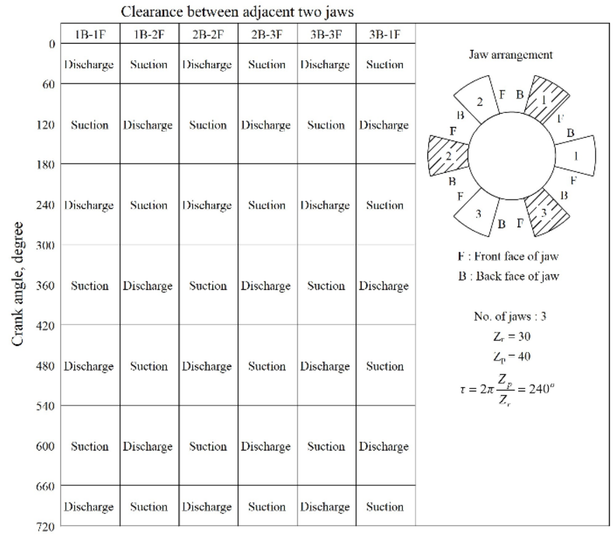

Fig. 6. A sequence of suction and discharge motions by the clearance angle between two adjacent jaws.

$$\left(\theta_{front}\right)_{\max} = \left(\theta_{rel}\right)_{\max} - \left(-\theta_{rel}\right)_{\max} = 2\left(\theta_{rel}\right)_{\max} \tag{15}$$

$$\left(\theta_{back}\right)_{\max} = \left(\theta_{rel}\right)_{\max} + \left(\theta_{rel}\right)_{\max} = 2\left(\theta_{rel}\right)_{\max} . \tag{16}$$

As the clearance angle increases from zero to the maximum, a sucking motion occurs between the two adjacent jaws. By contrast, as the clearance angle decreases from a maximum to zero, a discharge motion occurs. These suction and discharge motions occur as frequent as the number of clearances formed by the rotors during a period of $\tau = 2\pi \dfrac{Z_p}{Z_r}$. Fig. 6 illustrates a sequence of the suction and discharge motions that can be developed during one complete cycle of a rotary clap mechanism having 3-jaw rotors (N = 3), 20-tooth gear (Z_p = 20) and 30-tooth fixed internal gear (Z_r = 30).

Fig. 4 shows that the two rotors come in contact at crank angles of $\theta_c = \dfrac{\pi Z_p}{2Z_r}(2K-1)$, $K = 1, 2, 3, \cdots$. At these crank angles, r_{p1} and r_{p2} become equal, i.e.,

$$r_{p_1} = \sqrt{r_c^2 + \frac{L^2}{4} + r_c L \cos\frac{Z_r}{Z_p}\frac{\pi Z_p}{2Z_r}} = \sqrt{r_c^2 + \frac{L^2}{4}} \tag{17}$$

$$r_{p_2} = \sqrt{r_c^2 + \frac{L^2}{4} - r_c L \cos\frac{Z_r}{Z_p}\frac{\pi Z_p}{2Z_r}} = \sqrt{r_c^2 + \frac{L^2}{4}} \tag{18}$$

and θ_{rev} between r_{p1} and r_{p2} becomes

$$\theta_{rev} = \cos^{-1}\frac{r_{p_1}^2 + r_{p_2}^2 - L^2}{2 r_{p_1} r_{p_2}} = \cos^{-1}\frac{4r_c^2 - L^2}{4r_c^2 + L^2} . \tag{19}$$

Then, $\left(\theta_{rel}\right)_{\max}$ can be obtained as follows (Fig. 2):

$$\left(\theta_{rel}\right)_{\max} = \pi - \cos^{-1}\frac{4r_c^2 - L^2}{4r_c^2 + L^2} . \tag{20}$$

3.2 Velocity

As the crank rotates with a constant angular velocity, $\dot{\theta}_c$, the absolute angular velocity of the gear on the shaft link is obtained by taking the time derivative of Eq. (1) as follows:

$$\dot{\phi} = \left(1 - \frac{Z_r}{Z_p}\right)\dot{\theta}_c . \tag{21}$$

Differentiating the position vector Eq. (2) with respect to time yields

$$i r_c \dot{\theta}_c e^{i\theta_c} + i\dot{\phi}\frac{L}{2}e^{i\phi} - \dot{r}_{p_1} e^{i\theta_{p_1}} - i r_{p_1}\dot{\theta}_{p_1} e^{i\theta_{p_1}} = 0 . \tag{22}$$

Eq. (22) can be resolved into two Eqs. (23) and (24) by equating the real and imaginary parts. In other words,

$$-r_c\dot{\theta}_c \sin\theta_c - \frac{L}{2}\dot{\phi}\sin\phi - \dot{r}_{p_1}\cos\theta_{p_1} + r_{p_1}\dot{\theta}_{p_1}\sin\theta_{p_1} = 0 \tag{23}$$

$$r_c\dot{\theta}_c \cos\theta_c + \frac{L}{2}\dot{\phi}\cos\phi - \dot{r}_{p_1}\sin\theta_{p_1} - r_{p_1}\dot{\theta}_{p_1}\cos\theta_{p_1} = 0 . \tag{24}$$

Similarly, the following equations can be obtained from Eq. (3).

$$-r_c\dot{\theta}_c \sin\theta_c + \frac{L}{2}\dot{\phi}\sin\phi + \dot{r}_{p_2}\cos\theta_{p_2} - r_{p_2}\dot{\theta}_{p_2}\sin\theta_{p_2} = 0 \tag{25}$$

$$r_c\dot{\theta}_c \cos\theta_c - \frac{L}{2}\dot{\phi}\cos\phi + \dot{r}_{p_2}\sin\theta_{p_2} + r_{p_2}\dot{\theta}_{p_2}\cos\theta_{p_2} = 0 . \tag{26}$$

Solving Eqs. (23) and (24) for $\dot{r}_{p_1}$ and $\dot{\theta}_{p_1}$ gives velocities of pin P_1 and rotor 1 as

$$\dot{r}_{p_1} = -r_c\dot{\theta}_c \sin\left(\theta_c - \theta_{p_1}\right) - \frac{L}{2}\dot{\phi}\sin\left(\varphi - \theta_{p_1}\right) \tag{27}$$

$$\dot{\theta}_{p_1} = \frac{r_c\dot{\theta}_c\cos\left(\theta_c - \theta_{p_1}\right) + \dfrac{L}{2}\dot{\phi}\cos\left(\varphi - \theta_{p_1}\right)}{r_{p_1}} . \tag{28}$$

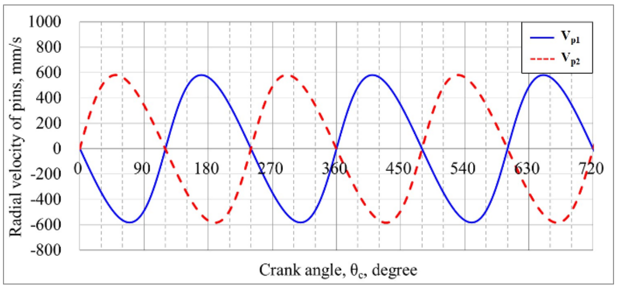

Fig. 7. Pin velocity when r_c = 5 mm, L = 40 mm, Z_r = 30, Z_p = 20 and $\dot{\theta}_c = 740\ rpm$.

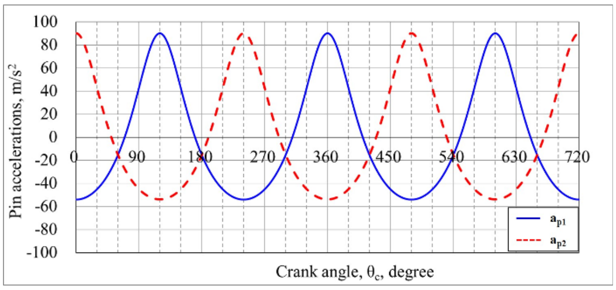

Fig. 9. Pin accelerations when r_c = 5 mm, L = 40 mm, Z_r = 30, Z_p = 20, and $\dot{\theta}_c = 740\ rpm$.

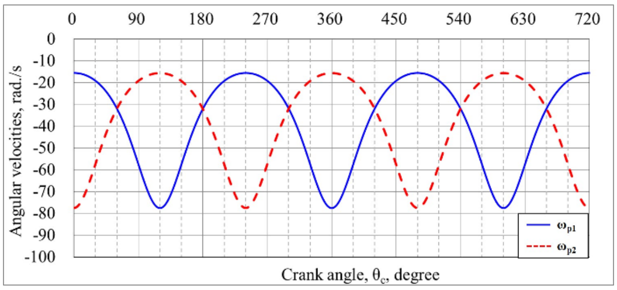

Fig. 8. Angular velocity of rotor when r_c = 5 mm, L = 40 mm, Z_r = 30, Z_p = , and $\dot{\theta}_c = 740\ rpm$.

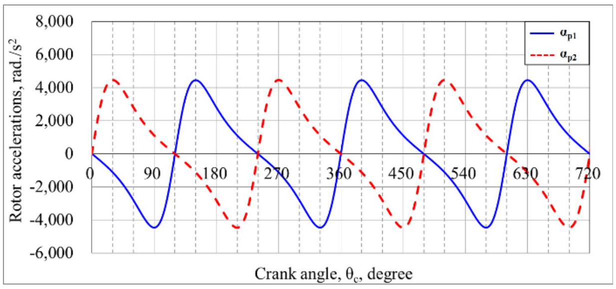

Fig. 10. Angular acceleration of rotors when r_c = 5 mm, L = 40 mm, Z_r = 30, Z_p = 20, and $\dot{\theta}_c = 740\ rpm$.

Similarly, velocities of pin P_2 and rotor 2, $\dot{r}_{P_2}$ and $\dot{\theta}_{P_2}$, are obtained from Eqs. (25) and (26) as follows:

$$\dot{r}_{P_2} = r_c\dot{\theta}_c \sin\left(\theta_c - \theta_{P_2}\right) - \frac{L}{2}\dot{\phi}\sin\left(\phi - \theta_{P_2}\right) \tag{29}$$

$$\dot{\theta}_{P_2} = \frac{-r_c\dot{\theta}_c \cos\left(\theta_c - \theta_{P_2}\right) + \frac{L}{2}\dot{\phi}\cos\left(\phi - \theta_{P_2}\right)}{r_{P_2}} . \tag{30}$$

Figs. 7 and 8 show $\dot{r}_{P_1}$, $\dot{r}_{P_2}$, $\dot{\theta}_{P_1}$ and $\dot{\theta}_{P_2}$ as a function of the crank angle during one complete cycle of the clap mechanism.

3.3 Accelerations

Accelerations of the pins and rotors are obtained by taking the time derivative of the velocity vector equations. Differentiating Eqs. (27) and (28) with respect to time and equating the real and imaginary parts yield a set of two simultaneous equations. Solving these equations for $\ddot{r}_{P_1}$ and $\ddot{\theta}_{P_1}$ gives the accelerations of pin P_1 and rotor 1 as follows:

$$\begin{aligned}\ddot{r}_{P_1} = & -r_c\ddot{\theta}_c \sin\left(\theta_c - \theta_{P_1}\right) - \frac{L}{2}\ddot{\phi}\sin\left(\phi - \theta_{P_1}\right) \\ & - r_c\dot{\theta}_c^{2} \cos\left(\theta_c - \theta_{P_1}\right) - \frac{L}{2}\dot{\phi}^{2} \cos\left(\phi - \theta_{P_1}\right) + r_{P_1}\dot{\theta}_{P_1}^{2}\end{aligned} \tag{31}$$

$$\ddot{\theta}_{P_1} = \frac{1}{r_{P_1}}\left\{\begin{aligned} & r_c\ddot{\theta}_c \cos\left(\theta_c - \theta_{P_1}\right) + \frac{L}{2}\ddot{\phi}\cos\left(\phi - \theta_{P_1}\right) \\ & -r_c\dot{\theta}_c^{2} \sin\left(\theta_c - \theta_{P_1}\right) - \frac{L}{2}\dot{\phi}^{2} \sin\left(\phi - \theta_{P_1}\right) \\ & -2\dot{r}_{P_1}\dot{\theta}_{P_1}\end{aligned}\right\} . \tag{32}$$

Similarly, the accelerations of the pin P_2 and rotor 2, $\ddot{r}_{P_2}$ and $\ddot{\theta}_{P_2}$, can be obtained from Eqs. (29) and (30). Thus,

$$\begin{aligned}\ddot{r}_{P_2} = & r_c\ddot{\theta}_c \sin\left(\theta_c - \theta_{P_2}\right) - \frac{L}{2}\ddot{\phi}\sin\left(\phi - \theta_{P_2}\right) \\ & + r_c\dot{\theta}_c^{2} \cos\left(\theta_c - \theta_{P_2}\right) - \frac{L}{2}\dot{\phi}^{2} \cos\left(\phi - \theta_{P_2}\right) + r_{P_2}\dot{\theta}_{P_2}^{2}\end{aligned} \tag{33}$$

$$\ddot{\theta}_{P_2} = \frac{1}{r_{P_2}}\left\{\begin{aligned} & -r_c\ddot{\theta}_c \cos\left(\theta_c - \theta_{P_2}\right) + \frac{L}{2}\ddot{\phi}\cos\left(\phi - \theta_{P_2}\right) \\ & +r_c\dot{\theta}_c^{2} \sin\left(\theta_c - \theta_{P_2}\right) - \frac{L}{2}\dot{\phi}^{2} \sin\left(\phi - \theta_{P_2}\right) \\ & -2\dot{r}_{P_2}\dot{\theta}_{P_2}\end{aligned}\right\} . \tag{34}$$

Notably, the accelerations $\ddot{\theta}_c$ and $\ddot{\phi}$ become zero if the angular velocity of the crank is constant. Figs. 9 and 10 show accelerations, $\ddot{r}_{P_1}$, $\ddot{r}_{P_2}$, $\ddot{\theta}_{P_1}$, and $\ddot{\theta}_{P_2}$ as a function of the crank angle when the crank rotates with a constant angular velocity.

4. Mechanism parameters

4.1 Parameters of driving links

Driving links of the rotary clap mechanism, which include the crank, the gears on the shaft link and the fixed internal gears, drive the rotors. The parameters of these links are related to each other as follows:

$$\frac{2r_c}{m} + Z_p = Z_r \tag{35}$$

where m is the gear module.

In addition to this relationship, the number of teeth on the gear in the shaft link and the fixed internal gear must satisfy the integer requirement that determines the relationship between the number of cycles for suction and discharge motions and the working period of the mechanism. In other words, the frequency of the suction and discharge motions during a working cycle of the mechanism must be an integer that completes the motions during the cycle. This relation can be expressed as follows:

$$N = \frac{Period\ \ for\ one\ working\ cycle\ of\ \ mechanism}{Period\ \ for\ suction\ and\ discharge\ motions} = \frac{\dfrac{2\pi Z_p}{Z_r - Z_p}}{\dfrac{2\pi Z_p}{Z_r}} = \frac{Z_r}{Z_r - Z_p}$$

$$\text{or} \quad \frac{NZ_p}{N-1} = Z_r \tag{36}$$

where N is an integer.

This equation also determines the number of jaws that should be mounted on the rotors and the suction and discharge ports. The driving links must satisfy Eqs. (35) and (36).

4.2 Rotor parameters

Rotor parameters describe the configuration of the rotors. They include the inner diameter, outer diameter and width of the rotor, number of jaws, pitch angle, thickness angle, height and width of the jaw, and length of the slot (Fig. 11).

From Eq. (36), the number of jaws is determined as N. Then, the pitch angle of the jaw, ψ, defined as an angle between the jaws is given by

$$\psi = \frac{2\pi}{N}. \tag{37}$$

To determine the thickness angle of the jaw, the maximum relative angular displacements between the rotors 1 and 2, i.e., $(\theta_{rel})_{\max} = (\theta_{p_1} - \theta_{p_2})_{\max}$, must be known. Let θ_t be the thickness angle of the jaw, then the maximum relative angular displacement can be expressed as

$$2(\theta_{rel})_{\max} = \frac{2\pi - N(2\theta_t)}{N}. \tag{38}$$

Substituting Eq. (20) into Eq. (38) and solving for the thickness angle of the jaw yields

$$\theta_t = \frac{\pi}{N} - \left(\pi - \cos^{-1}\frac{4r_c^2 - L^2}{4r_c^2 + L^2}\right). \tag{39}$$

The inner radius of the rotor should be smaller than the minimum value of r_{p1} or r_{p2}, and the outer radius should be larger than the maximum value of r_{p1} or r_{p2}, which all depend on the values of r_c and L. The length of the slot, s, on the rotor also depends on the values of r_c and L, and is given in equation form as follows:

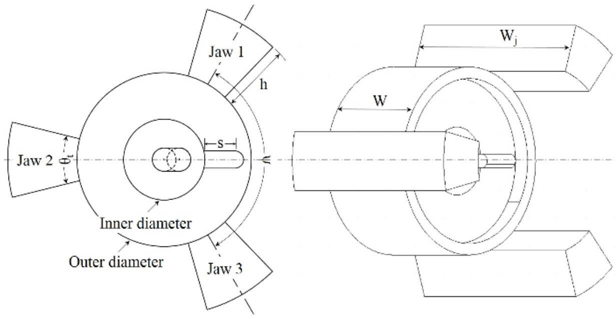

Fig. 11. Rotor parameters.

$$s = (r_{p_1})_{\max} - (r_{p_1})_{\min} = \sqrt{r_c^2 + \frac{L^2}{4} + r_c L} - \sqrt{r_c^2 + \frac{L^2}{4} - r_c L}. \tag{40}$$

The width of jaw, W_j, should be twice the rotor width, W.

5. Performance parameters

Displacement and flow may be the most important parameters to evaluate the performance of the rotary clap mechanism as a pumping device. During the suction motion, the volume, V, displaced by the two adjacent jaws can be expressed as

$$V = \pi\left[(r_o + h)^2 - r_o^2\right] W_j \frac{(\theta_{front})_{\max}}{2\pi} \tag{41}$$

where r_o is the outer radius of rotor, h is the jaw height, and W_j is the jaw width.

When the crank completes one revolution, the number of cycles for the suction and discharge motions become

$$\frac{2\pi}{2\pi\dfrac{Z_p}{Z_r}} = \frac{Z_r}{Z_p}.$$

Therefore, the displacement of the clap pump mechanism can be expressed as

$$D = \pi\left[(r_o + h)^2 - r_o^2\right] W_j \frac{(\theta_{front})_{\max}}{2\pi}\left(\frac{Z_r}{Z_p}\right)(2N). \tag{42}$$

If the crank rotates at a constant angular velocity of $\dot{\theta}_c$ rpm, the theoretical mean flow of the rotary clap pump can be calculated as follows:

$$Q_{avg} = \pi\left[(r_o + h)^2 - r_o^2\right] W_j \frac{(\theta_{front})_{\max}}{2\pi}\left(\frac{Z_r}{Z_p}\right)(2N)\dot{\theta}_c. \tag{43}$$

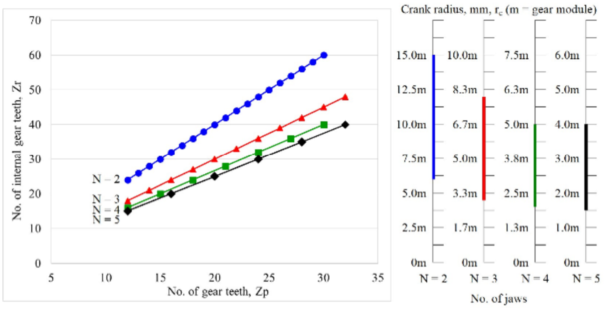

Fig. 12. Determination of the number of internal gear teeth and crank radius by the number of the gear teeth and rotor jaws.

6. Interrelations of parameters

To evaluate the performance characteristics of the rotary clap mechanism as a pumping device, the effects of a number of mechanism parameters on the displacement were investigated. As shown in Eqs. (15), (20) and (42), displacement of the rotary clap mechanism is primarily affected by the number of jaws, crank radius, pin distance, and number of teeth on the gears. However, identification of unique effects of these parameters on the displacement is difficult because these parameters are inter-related.

From Eqs. (35) and (36), the crank radius and number of the fixed internal gear teeth can be obtained from the number of the gear teeth on the shaft link and rotor jaws (Fig. 12).

Another constraint that limits the crank radius is the thickness angle of the jaw. The thickness angle is affected by the crank radius, number of rotor jaws, and pin distance. The thickness angle should be positive and greater than a given value; thus, the crank radius must be determined under such a constraint. Fig. 13 shows the positive thickness angles that can be obtained by the combinations of the crank radius, number of rotor jaws, and pin distance. As the number of jaws increases, the crank radius must be reduced to obtain the positive thickness angle (Fig. 13). If necessary, the crank radius can be increased by increasing the pin distance. However, increasing the crank radius is limited because the thickness angle becomes negative as the crank radius increases regardless of the pin distance. Therefore, the crank radius must be determined to satisfy the lower limit required to drive the mechanism, taking the number of jaws and the pin distance into consideration.

The crank radius and pin distance are also affected by the minimum and maximum radii of the pin rotation with respect to the center of the rotor, from which the inner and outer radii of the rotor can be determined. The maximum rotating radius of the pin increases with the crank radius and pin distance, whereas the minimum rotating radius increases only with the pin distance but decreases with the crank radius (Figs. 14 and 15). The maximum and minimum rotating radii of the pin also determine the length of the slot on the rotor face as shown in Eq. (40).

Notably, the inner radius of the rotor must be less than the

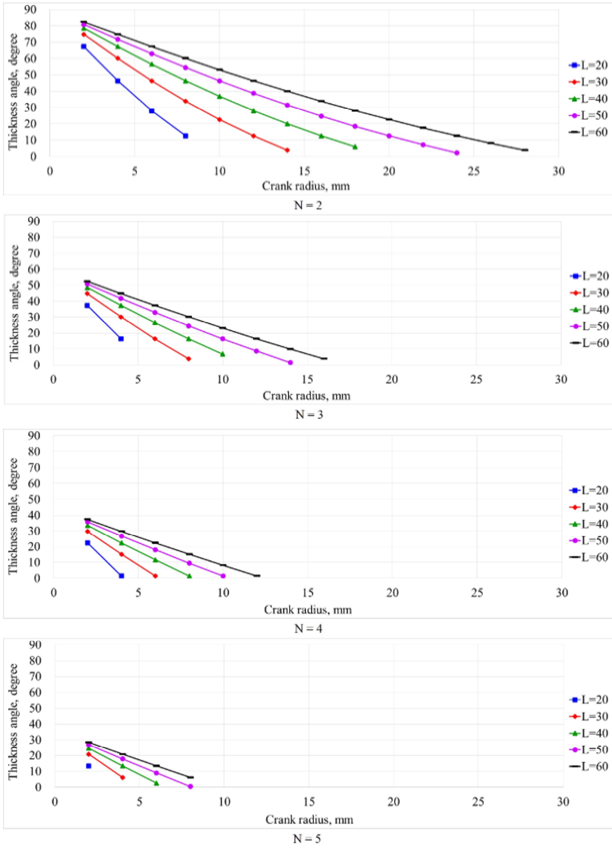

Fig. 13. Combinations of crank radius, number of rotor jaws, and pin distance for positive thickness angles.

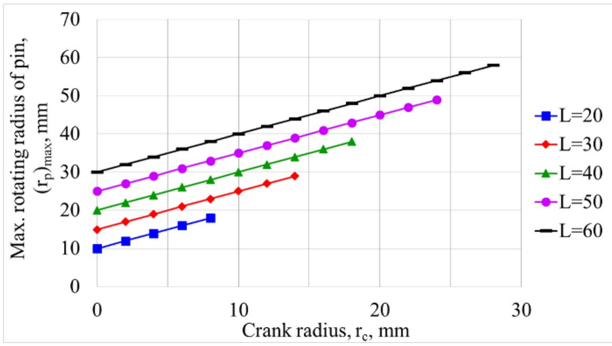

Fig. 14. The maximum rotating radius of the pin.

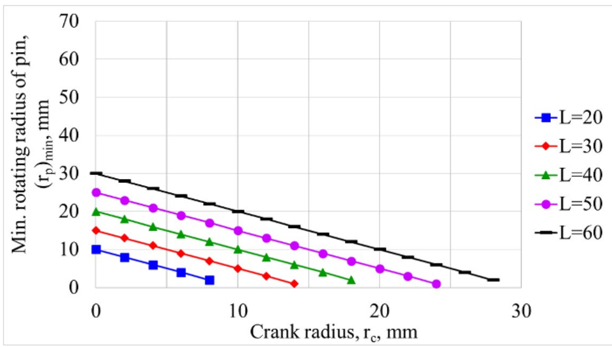

Fig. 15. The minimum rotating radius of the pin.

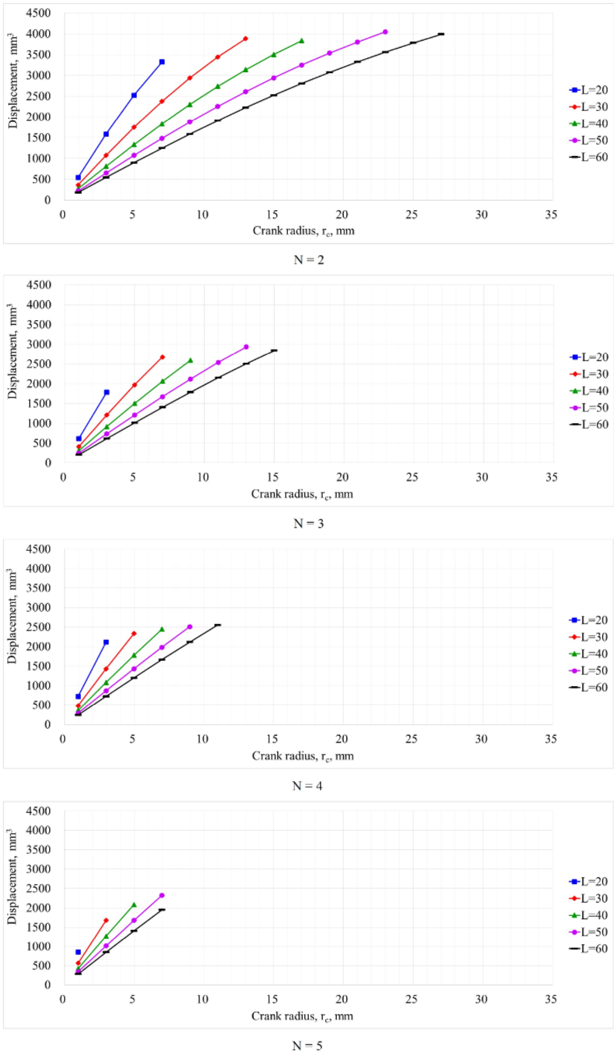

Fig. 16. Displacement of the clap mechanism having a jaw with 50 mm width and 40 mm height and a rotor with 65 mm outer radius.

minimum rotating radius of the pin, whereas the outer radius must be greater than the maximum rotating radius.

The crank radius and pin distance are limited by the thickness angle of the jaw and the inner radius of the rotor; thus, they must be determined within the allowable range of the overall size of the clap mechanism. Once the crank radius and pin distance are determined, the number of gear teeth and its module can be determined accordingly using Fig. 12.

7. Performance characteristics

Displacement of the clap mechanism varies with crank radius, pin distance, number of jaws, and jaw width and height. Fig. 16 shows the displacement of the mechanism when the width and height of jaw are kept constant with a rotor of 65 cm outer radius. Displacement increases with the crank radius at a given number of jaws and pin distance. However, at a given crank radius, it increases with the number of jaws and decreases with the pin distance. The crank radius is limited as the number of jaws increase; thus, the displacement performance of the clap mechanism is also limited by the number of jaws. However, it can be optimally increased by increasing the jaw width and height once the crank radius, pin distance, and the number of jaws are determined because they are not inter-related with other parameters of the mechanism.

8. Conclusions

A five-bar spatial mechanism named a rotary clap mechanism was developed as a pumping device for positive displacement rotary pumps. The mechanism was intended to convert the reciprocating piston pump into a rotary version that will reduce the high level of vibration and power losses of piston pumps caused by excessive friction between the reciprocating piston and pump housing as the pumping speed increases.

The mechanism comprises a driving crank, a shaft link having two pins and two gears mounted on the middle and both ends, respectively, two rotors with equally spaced jaws along their circumferences, and a fixed internal gear. The crank drives the shaft link through the gears so that the pins on the shaft link simultaneously rotates about the crank pin and about the center of the fixed internal gear, which periodically varies the radius of rotation of the pin about the center of the fixed internal gear. The two rotors driven by the pins, therefore, rotate with different angular velocities as the crank rotates at constant velocity. One rotor alternately leads and lags relative to the other. These lead and lag motions between two adjacent jaws of the rotors result in suction and discharge motions required for pumping.

The working principle of the rotary clap mechanism and its design parameters were introduced together with the kinematic analysis for the pins and rotors. Vector equations developed for the analysis can be used to easily depict the motion characteristics of the mechanism by changing the design parameters. The relationships among the design parameters were also presented to determine the proper crank radius and pin distance within the allowable number of gear teeth and rotor size. The thickness angle of the jaw and inner radius of the rotor were the most significant constraints affecting the crank radius and pin distance of the mechanism.

The displacement of the clap mechanism varies with crank radius, pin distance, number of jaws, jaw width, and jaw height. It increases with the crank radius at a given number of jaws and pin distance, whereas it decreases with pin distance and increases with the number of jaws at a given crank radius. However, the displacement can be optimally increased by increasing the jaw width and height once the crank radius, pin distance, and the number of jaws are determined because they are not inter-related with other parameters of the mechanism.

The rotary clap mechanism can be applied to a pumping device despite a number of limitations caused by constraints on the crank radius and pin distance.

References

[1] A. J. Shih, Kinematics of the cycloidal internal combustion engine mechanism, *J. Mech. Des. ASME,* 115 (4) (1993) 953-959.
[2] A. J. Shih, Analysis and comparison of epicycloidal and hypocycloidal internal combustion engine mechanisms, *J. Mech. Des. ASME,* 115 (4) (1993) 960-966.
[3] B. V. Librovich and A. F. Nowakowski, Analysis, design, and modeling of a rotary vane engine (RVE), *J. Mech. Des. ASME,* 126 (4) (2004) 711-720.
[4] B. V. Librovich, Dynamics of rotary vane engine, *J. Mech. Des. ASME,* 125 (3) (2003) 498-508.
[5] E. F, Drachko, *Rotary piston machine of volumetric expansion*, Russian patent, 2439333 (2006).
[6] H. Deng, C. Pan, X. Xu and X. Zhang, A twin-rotor piston engine with annular connecting chambers, *Proceedings of Institution of Mechanical Engineers, Part C: J. Mech. Eng. Sci.,* 227 (5) (2013) 1080-1089.
[7] J. M. Kim, *Dual unequal rotational volumetric suction and discharging device*, Korean patent, 101073159 (2011).
[8] J. M. Kim, *Rotational clap suction/pressure device*, PCT KR2012001710 (2012).
[9] M. Sakita, A cat-and-mouse type rotary engine: engine design and performance evaluation, *Proceedings of Institution of Mechanical Engineers, Part C: J. Mech. Eng. Sci.,* 220 (8) (2006) 1139-1151.
[10] G. M. Ralph, *Internal combustion engine and method*, US patent, 6 739 307 B2 (2004).
[11] X. Xu, A cam-quadrilateral mechanism for power transmission of a twin-rotor piston engine, *Journal of Mechanical Science and Technology*, 28 (3) (2014) 953-961.

Sung Bo Shim holds a B.S. and an M.S. degrees in Biosystems Engineering from Seoul National University, Korea. He is currently a doctoral candidate in Biosystems Engineering at Seoul National University. He is interested in off-road vehicles and durability tests of machine components.

Young Jun Park has been working in Korea Institute of Machinery & Materials (KIMM) in Daejeon, Korea since 2006. He is interested in the design and analysis of gearboxes and bearings for wind turbines and construction equipment. He received a B.S., an M.S., and a Ph.D. degrees in Agricultural Machinery Engineering from Seoul National University, Korea.

Jong Mun Kim is currently the CEO of ClapMC Co. at Deajeon, Korea. He is interested in rotary machines (e.g., engine, expander, pump, etc). He has Korean patents for rotary clap mechanism. He holds a B.S. degrees in Agricultural Engineering from Seoul National University.

Kyeong Uk Kim has been a professor of Biosystems and Biomaterial Science and Engineering at Seoul National University, specializing in farm power and machinery, soil-machine systems, and life test of machine components. He has co-authored several books, including one that focuses on the principle of agricultural machines. He holds a B.S. and an M.S. degrees in Agricultural Engineering from Seoul National University and a Ph.D. in Agricultural Engineering from the University of Illinois at Urbana-Champaign, USA (1981).